Journal of Power Sources 210 (2012) 286–291

Contents lists available at SciVerse ScienceDirect

Journal of Power Sources

journal homepage: www.elsevier.com/locate/jpowsour

# Effects of undercharge and internal loss on the rate dependence of battery charge storage efficiency

Elena M. Krieger, Craig B. Arnold*

*Department of Mechanical and Aerospace Engineering, Princeton University, Princeton, NJ 08544, USA*

ARTICLE INFO

*Article history:*
Received 5 December 2011
Received in revised form 9 March 2012
Accepted 12 March 2012
Available online 22 March 2012

*Keywords:*
Battery charge efficiency
Ragone plot
Energy–power relationship
Li-ion battery

ABSTRACT

Battery charge efficiency across a range of input powers is an important performance parameter in variable charging systems. Here we use equivalent circuit theory to model the inherent trade-off between battery charging power and energy stored and compare our model to the existing Ragone model for discharge power and energy. An additional parameter is included to account for undercharge and underdischarge of the battery due to premature arrival at the battery's voltage limits. At a given power, energy efficiency is predicted to be higher for charging than discharging when only accounting for energy dissipated by internal resistance. We experimentally determine charge and discharge energy–power curves for lithium-ion batteries and find they exhibit a reduction in energy stored or withdrawn as power increases. We isolate the effects of undercharge and underdischarge from energy lost to internal resistance, and find the former outweighs the latter effect. Furthermore, the shallow shape of the voltage curve near the charge voltage cutoff results in a more limited range of charging powers than discharging powers. The model is expected to help inform operational parameters for battery charging for variable power sources.



## 1. Introduction

The time and efficiency of battery charging, much like for battery discharging, are becoming increasingly important parameters in evaluating battery performance due to the rising prevalence of applications with variable power sources, like solar and wind systems and regenerative braking in cars. New battery chemistries and control systems are rapidly being developed to meet the requirements of this evolving set of demands [1,2]. One distinctive feature of such systems is that battery charge profiles are not always predetermined [3,4]. Most commercial batteries, in contrast, are designed to be charged at a designated rate and discharged according to a given variable load. The charge procedure is typically a combination of constant current and constant voltage steps, with specific parameters and alternative techniques like pulse charging dependent on the chemistry of the battery [5]. However, in an increasing number of applications, batteries are charged by a variable current due to semi-stochastic power generation. Such applications include renewable electricity generation in wind and solar systems [3], charging of car batteries in electric and hybrid vehicles [4,6], or load-leveling in grid-level applications [7]. Battery charge power may vary significantly across these applications, but research on the dependence of battery efficiency on charge rate is typically focused on using a variable input to improve efficiency [5,8,9]. A few studies have evaluated the response of batteries over a range of charging powers [10,11], but further research is required to understand the relationship between charge and discharge behavior and the predominant factors contributing to this response. Battery charge efficiency cannot be considered a simple inverse of battery discharge efficiency, but we can use our understanding of discharge to better model charging efficiency across the wide range of input powers seen in non-optimized charging regimes.

The relationship between the energy available in a battery and discharge power has been well explored and is typically presented in a Ragone plot [12]. Ragone plots characteristically demonstrate that the specific energy of an electrochemical energy storage device decreases as a function of specific power. Ragone plots can be used to illustrate the admissible discharge range of a given battery as well as to compare optimal operational ranges for multiple energy storage devices and provide an elegant visualization of battery discharge efficiency. The fundamental basis for the trade-off between discharge energy and discharge power has been modeled by Christen and Carlen [13], and Christen and Ohler have described how this analysis can be used to optimize energy storage device selection [14].

Battery charge efficiency, defined here as the percent of energy stored by a battery charged at a given power for a unit of time, is also known to have a dependence on charge power [9–11,15]; the impact of this dependence on efficiency is particularly consequential in variable power systems [8]. Wang has used equivalent

* Corresponding author. Tel.: +1 617 258 1089; fax: +1 617 258 5877.
*E-mail address:* cbarnold@princeton.edu (C.B. Arnold).

0378-7753/$ – see front matter © 2012 Elsevier B.V. All rights reserved.
doi:10.1016/j.jpowsour.2012.03.029

circuits to demonstrate that the amount of energy lost during charging is dependent on power, and has used this relationship to develop a model for improving battery charge efficiency given time and power constraints [10]. These studies attribute the loss of energy at high powers to an increase in internal resistance losses at high current densities, yielding the characteristic Ragone curve shape in the discharge case. Verbrugge and Ying [11] further incorporated an equivalent circuit model with experimental voltage curves to model the capacity of lithium-ion batteries when charged and discharged over a range of powers and temperatures. Although these studies provide initial insight into the energy–power relationship for battery charging, it is of interest to better understand the difference between charge and discharge curves and determine the factors contributing to this behavior in order to improve battery charge efficiency and control systems across a range of applications.

In this paper, we aim to refine the existing framework for understanding battery charging by examining the relationship between charging and discharging and analyzing the factors leading to the energy–power relationship in both cases. We use an equivalent circuit-based model to describe the relationship between charge power and efficiency in order to expand upon and complement existing models of discharge behavior. Such a model will allow us to provide a functional form for the energy that can be drawn from a battery as function of charge or discharge power. We further separate the model into internal resistance effects and the impact of loss of available capacity due to premature arrival at voltage limits at high powers and experimentally determine the magnitude of these two effects in lithium-ion batteries. Such a theory will help us parameterize the available operating ranges of a battery and the effect a distribution of charge powers will have on storage efficiency. In the first two sections of this paper, we provide background on the equivalent circuit model and build on it to create a model for battery charge behavior. In the next section we present our experimental methods and finally we extract parameters from our experimental results and incorporate them into our model.

## 2. Battery charge model

### 2.1. Background

Ragone behavior has been modeled using equivalent circuit theory by Christen and Carlen [13]. Battery power ($P$) is represented by an RLC circuit governed by the following ODE with respect to time:

$$L\ddot{Q} + R\dot{Q} + V(Q) = -\frac{P}{\dot{Q}}, \tag{1}$$

where $L$ is internal inductance, $Q$ is charge, $R$ is internal resistance, and $V$ is voltage. Battery power at current $I$, in the simple case where inductance is considered negligible, is given by:

$$P = VI = (V_0 - IR)I. \tag{2}$$

The output voltage $V$ is offset from the cell voltage $V_0$ by an internal resistance loss $\Delta V = IR$. Eq. (2) can be rearranged to yield a charging current of:

$$I = \frac{V_0}{2R} \pm \sqrt{\frac{V_0^2}{4R^2} - \frac{P}{R}}. \tag{3}$$

The energy stored in the battery is given by $E_0 = Q_0 V_0$, where $Q_0$ represents the full charge available in the cell. The battery discharge time $t_\infty = Q_0/I$ allows the energy drawn from the battery to be written as:

$$E = P\left(\frac{Q_0}{I}\right). \tag{4}$$

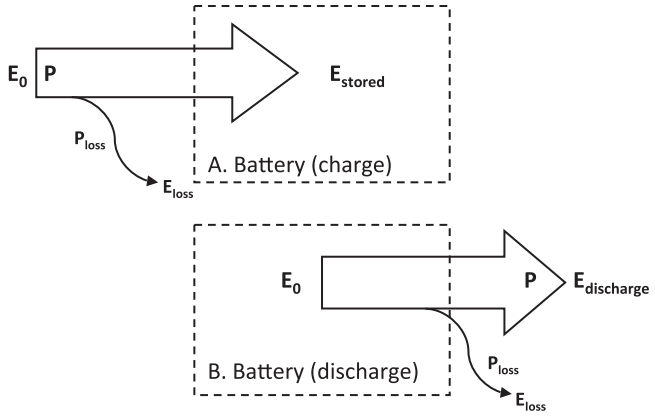


**Fig. 1.** Diagrams of batteries on (A) charge and (B) discharge show relative locations of power $P$, initial energy $E_0$ and energy stored or discharged.

Combining these two equations and using the dimensionless units $e = E/Q_0V_0$ and $p = 4RP/V_0^2$, as well as introducing a leakage resistance $R_L$, Christen and Carlen model the energy that can be drawn from the battery using the following governing equation:

$$e_d(p) = \frac{1}{2}\left(\frac{p}{1 - \sqrt{1-p} + 2(R/R_L)}\right). \tag{5}$$

This curve exhibits the experimentally established characteristic shape of a Ragone plot.

### 2.2. Energy–power charge curves

We model the relationship between energy and power during battery charging using a similar approach to the Christen and Carlen model but we account for three additional considerations. The first distinguishing feature is that this relationship cannot be modeled by taking the opposite sign for power used in the discharge model. When modeling discharge energy and power, both of these variables are measured at the same location, namely as an output from the battery. However, in the charge case, we are interested in evaluating how much energy is stored inside the battery as a function of an external input power. We can compare both charge and discharge efficiency by taking an initial amount of energy $E_0$ and asking how much of this energy is stored or discharged at a given power. A normalized Ragone plot reflects energy efficiency by illustrating the percent of $E_0$ that can be drawn from a battery at a given discharge power $P$. To create a comparable model for the battery charge case, we similarly ask what percent of a given initial energy $E_0$ will be stored in a battery if charged at a power $P$. The relative definitions of power $P$, initial energy $E_0$ and energy stored or discharged can be visualized in Fig. 1. By using these definitions, we can compare charge and discharge efficiency as a function of power. If instead we had reversed the sign on power, we would be asking the question of how much energy would be required to reach full charge at a given charge power; in the high power limit, energy input would approach infinity and our model would be illustrating energy demand instead of energy efficiency.

The second differentiating feature of our approach is the introduction of another level of complexity to the discharge model. The original model assumes that the battery has a constant cell voltage and therefore constant discharge current for a given power. However, battery voltage varies with state of charge; current must therefore also vary to maintain a constant power. This behavior can be accounted for by integrating over voltage and current curves if they have been experimentally determined or previously modeled for a given chemistry, in a similar fashion to prior work [11].

Finally, in practice, most batteries are charged or discharged until a voltage limit is reached. Beyond this limit, the cell may suffer from irreversible damage to the electrodes. These cutoffs are reached prematurely at high currents due to the increased impact of the internal resistance offset on cell voltage. This effect results in undercharge (or underdischarge), which reduces total Ah throughput. Undercharge and underdischarge can be represented as a change in total charge stored in or drawn from the battery, whereas the typical Ragone model describes a reduction in energy efficiency due to internal resistance. We will represent undercharge and underdischarge separately to ultimately determine the magnitude of their contribution to the typical Ragone shape. We therefore define the total available capacity at a given power as $Q(P)$, with a maximum of $Q_0$ when $I \to 0$. We will extract a functional value for $Q(P)$ in Section 3.

Taking these parameters into consideration, we aim to model $E_C(P)$, the energy stored in the battery as a function of charge power. Battery voltage $V$ is a function of state of charge $q$, so at a constant power, current $I$ must also vary as a function of $q$. Additionally, internal resistance and impedance have been shown to be a function of state of charge [16,17]. The input power is therefore described by:

$$P = I(q)(V(q) + I^2(q)R(q)). \tag{6}$$

The first term in Eq. (6) describes the amount of power used to directly store energy in the battery at state of charge $q$:

$$P_{\text{internal}}(q) = I(q)V(q). \tag{7}$$

The second term describes the power dissipated as heat loss:

$$P_{\text{loss}}(q) = I^2(q)R(q). \tag{8}$$

The input energy $E_0$, or the amount of energy stored in the battery in the limit of no loss, can be found by integrating voltage over all states of charge:

$$E_0 = \int_0^{Q_0} V(q)dq. \tag{9}$$

The total energy stored can be found by subtracting the energy lost to internal resistance from the total initial energy according to:

$$E_C(P) = E_0 - \langle P_{\text{loss}}(P)\rangle \; t_\infty(P). \tag{10}$$

The average loss at a given charge power can be written:

$$\langle P_{\text{loss}}(P)\rangle = \frac{\int_0^{Q(P)} I^2(q)R(q)dq}{Q(P)} \tag{11}$$

and the total charge time is:

$$t_\infty(P) = \frac{Q(P)}{\langle I\rangle} = \frac{Q^2(P)}{\int_0^{Q(P)} I(q)dq}. \tag{12}$$

The amount of energy stored as a function of input power becomes:

$$E_C(P) = \int_0^{Q_0} V(q)dq - \frac{Q(P)\int_0^{Q(P)} I^2(q)R(q)dq}{\int_0^{Q(P)} I(q)dq}. \tag{13}$$

We can rearrange Eq. (6) to find the following equation for current as a function of power and state of charge:

$$I(q,P) = -\frac{V(q)}{2R(q)} \pm \sqrt{\frac{V^2(q)}{4R^2(q)} + \frac{P}{R(q)}}. \tag{14}$$

We will take the positive limit for $I$ which yields the limit $I \to 0$ as $P \to 0$. If the functional form for $V(q)$ has been determined, as has been done for nickel-metal hydride, polymer lithium ion [18], lithium-ion [19], lead-acid [20], and most other commercial batteries, these equations can be substituted into Eqs. (13) and (14) and numerically solved to determine $E(P)$.

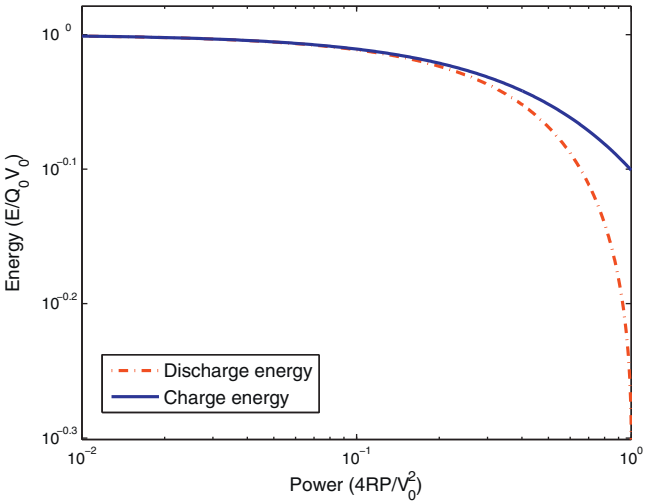


**Fig. 2.** The energy–power relationship for batteries is plotted in dimensionless units. Energy loss due to internal resistance is higher for discharge than charge at high powers.

In the idealized case voltage and resistance are not dependent on state of charge $q$ so we can eliminate the integrals and use constant values for open circuit voltage $V(q) = V_0$ and internal resistance $R(q) = R_0$. By looking at this case, we can write the equation for charge energy as a function of power as:

$$E_C(P) = Q_0V_0 + \left(\frac{V_0}{2R_0} - \sqrt{\frac{V_0^2}{4R_0^2} + \frac{P}{R_0}}\right)Q(P)R_0. \tag{15}$$

As would be expected, $E(P) \to E_0$ in the limit where $P \to 0$.

The degree of undercharge and underdischarge, as reflected in $Q(P)$, will be experimentally determined for a lithium-ion battery in Section 4. We first will look at the case where there is no undercharge nor underdischarge and therefore we can assume the battery reaches maximum charge $Q(P) = Q_0$. At this limit, we can introduce the same dimensionless units as Christen and Carlen $e_c = E_C/Q_0V_0$ and $p = 4R_0P/V_0^2$, yielding the following dimensionless curve for energy as a function of power:

$$e_c(p) = \frac{3}{2} - \frac{1}{2}\sqrt{1+p}. \tag{16}$$

From Eq. (5) in the Christen and Carlen model [13], we know discharge energy as a function of power, in the case of no leakage (or infinite leakage resistance), can be written:

$$e_d(p) = \frac{1}{2} + \frac{1}{2}\sqrt{1-p}. \tag{17}$$

Fig. 2 plots normalized charge energy and discharge energy as a function of power. The result suggests that at any given power a smaller percentage of energy is lost to internal resistance upon charge than upon discharge; we attribute this effect to the lower current (higher charging voltage) and therefore lower IR loss at a given power in the charge case. The ideal battery considered here therefore has a larger operational range of charging powers than discharging powers, although as we will see other practical features outweigh this effect. The difference in energy loss between these curves is given by:

$$e_{diff} = 1 - \frac{1}{2}\left(\sqrt{1-p} + \sqrt{1+p}\right). \tag{18}$$

We have neglected leakage currents in this model. Leakage is an important determinant of capacity retention during battery storage, and may affect very low charge currents, but its impact is minimal at most standard C-rates. Furthermore, the model does

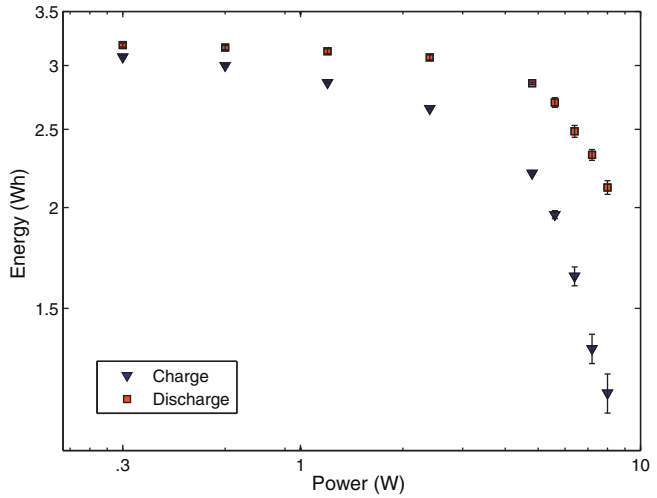


**Fig. 3.** Energy–power curves for lithium-ion cells. Charging exhibits a more limited power range than discharging.

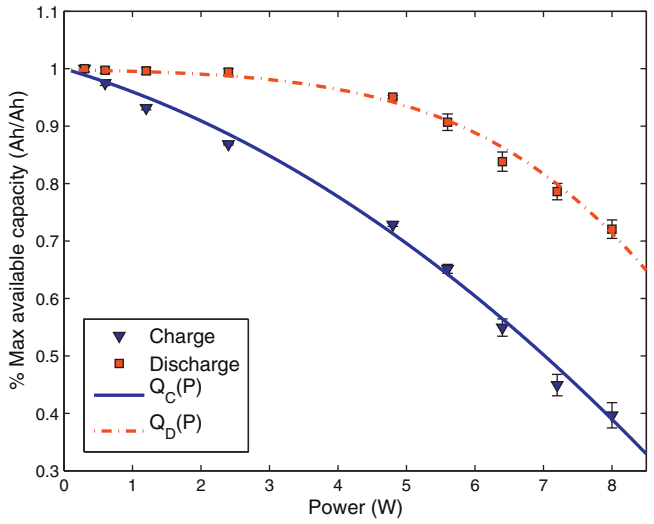


**Fig. 4.** Undercharge and underdischarge as a function of power. The available capacity in the cell is shown as a percent of maximum charge as a function of power. The fit to these curves yields $Q(P)$.

not explicitly include the detailed thermodynamics of charging and discharging; these details are implicitly included through the resistance and voltage functions which are experimentally measured.

## 3. Experimental

To validate the energy–power relationship for battery charging and to experimentally extract a functional form for $Q(P)$, 900 mAh Tenergy lithium-ion 14500 cells are cycled on an Arbin BT 2000 battery tester. All tests are carried out at room temperature (~23 °C). Battery capacity is determined using the manufacturer's charging protocols and found to range from 820 mAh to 830 mAh. A Ragone plot is generated by charging each cell at $C/5$ to 4.2 V, maintaining constant voltage until current drops below 0.01 A, resting at open circuit for 10 min, and discharging at constant power to 2.75 V. Power ranges from 0.3 W to 8.0 W. A charge power–energy plot is generated by charging cells at constant power (0.3–8.0 W) to a cut-off voltage of 4.2 V, resting 10 min, and discharging at a $C/5$ current to 2.75 V. The low C-rate discharge current is selected to minimize efficiency losses on discharge; although some losses are to be expected, we assume minimal variation in the efficiency of discharge across all cycles. The $C/5$ discharge rate is further considered sufficiently low so as to not contribute significantly to the underdischarge effect. All tests are repeated three times on two cells. Reported energy values are an average of the three cycles on two batteries.

## 4. Results and discussion

The total energy stored in and withdrawn from the experimental lithium-ion cells is plotted as a function of charge and discharge power in Fig. 3. These curves exhibit the characteristic trade-off between energy and power for both charge and discharge cases. The plots have different maximum energy values because the discharge tests reach a fuller capacity due to the constant voltage charging step. The charge plot exhibits a more rapid decline in efficiency at high powers than the discharge plot.

We expect the curve shape to be impacted by both internal resistance losses and by undercharge or underdischarge; these latter effects are reflected in the $Q(P)$ term in our model. In order to isolate each component, we find a functional form for the available capacity, $Q(P)$, so we can measure the contribution of undercharge and underdischarge to our results. The total charge stored in or drawn from the battery, $Q(P)$, can be experimentally determined by measuring the total Ah throughput before the voltage cutoff is reached. We find the maximum capacity $Q_0$ by measuring Ah throughput at a $C/5$ charge rate, which we determine to be a sufficiently low current for capacity to plateau.

Fig. 4 plots the available capacity of the battery in dimensionless units as a function of power; the Ah throughput is divided by the maximum capacity $Q_0$ to determine the available capacity as a percentage of the maximum. The charge plot exhibits a stronger dependence of available capacity on power than the discharge plot, indicating that undercharge has a greater magnitude than underdischarge in these batteries. We can fit these curves to functional forms, letting $Q_0$ be the maximum available capacity in the cell.

$$Q_D(P) = \tanh\left(\frac{12 - P}{\sqrt{P + 12}}\right)Q_0. \tag{19}$$

$$Q_C(P) = (1 - 0.035P - 0.0052P^2)Q_0 \tag{20}$$

Although the fits for $Q(P)$ are somewhat arbitrary, the term $(12 - P)$ in the discharge fit suggests that the maximum discharge power for these cells is near 12 W.

The larger magnitude of undercharge in Fig. 4 can be attributed to the location of the voltage cutoffs on the charge and discharge curves of these cells. This cutoff voltage occurs on a very steep section of the discharge curve, so a large $IR$ offset at high powers shifts the cutoff further up the steep slope but has little impact on total charge. Conversely, the cutoff voltage on the charge curve is located closer to a shallow section of the curve, so a small vertical offset can have a large horizontal impact on the cutoff location, resulting in a larger magnitude of undercharge. This effect is described with the voltage curves in Fig. 5. The voltage limit is indicated, as well as the location of the cutoff if the voltage offset increases by 0.2 V due to a power increase. Such an increase would shift the charge curve up and the discharge curve down, resulting in the indicated changes in the relative locations of the voltage cutoffs on the charge and discharge curves. The change in the Ah throughput is negligible for discharge with a 0.2 V offset, but Ah throughput is markedly decreased for the charge curve.

The open circuit voltages of the cells at the end of each half cycle provide an alternative measure of undercharge and underdischarge. Fig. 6 plots OCV at the end of each half cycle as a function of power. The rising OCV on discharge suggests that the battery is not fully discharged and operating primarily in higher states-of-charge. Similarly, the decreasing OCV on charge is

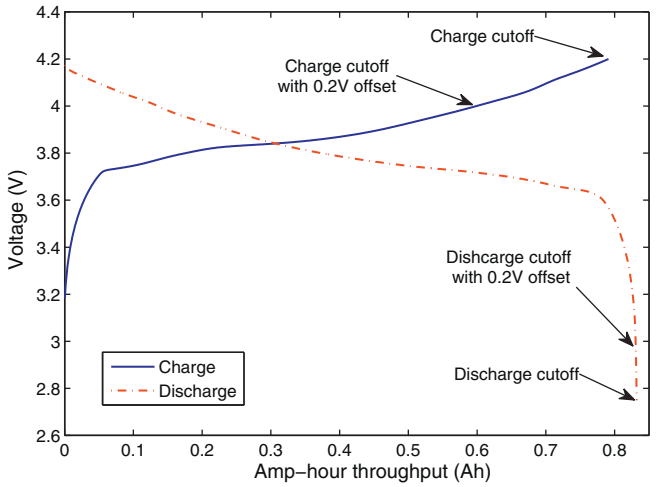


**Fig. 5.** Voltage curves at low power as a function of Ah of charge or discharge. The change in voltage cutoff location due to a 0.2 V internal resistance offset is indicated to show the greater loss in charge capacity than discharge capacity.

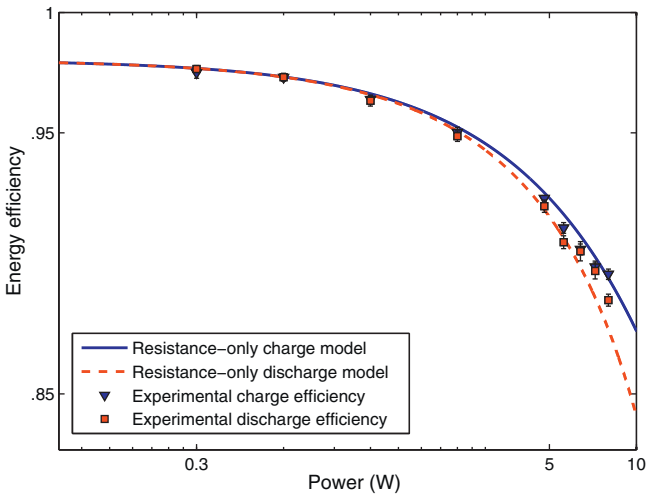


**Fig. 7.** Capacity-normalized energy–power curve with model overlay. The effect of undercharge and underdischarge is removed, and the resultant plot shows the impact of internal resistance loss on energy efficiency.

indicative of the battery not reaching full charge and operating primarily in lower states-of-charge. Both results confirm a large magnitude of undercharge and underdischarge. The OCV voltage after discharge changes disproportionately with power due to the steep shape of the discharge curve shown in Fig. 5.

In order to evaluate the contribution of internal resistance to the shape of the energy power curves, we remove the effect of underdischarge and undercharge by plotting the energy efficiency of each step as a function of power in Fig. 7. By examining $E_{out}/E_{in}$ we can determine the percent of energy lost during charge or discharge isolated from the effect of reduced available capacity at high powers. Our curves once again exhibit the characteristic energy–power shape, but the magnitude is much smaller than before. The discharge efficiency at a 10 C rate averages 88.5%, while the charge efficiency at 10 C averages 89.5%. We should point out that the intercept for the maximum efficiency at low powers reaches 98%, which suggests that the opposite half cycle of the one being tested (i.e. discharge on the charge cycle) is contributing to a small loss in efficiency due to a non-zero C-rate. The discharge cycles exhibit a lower efficiency than the charge cycles, as predicted by our model, but the difference is within the noise in the data for most points.

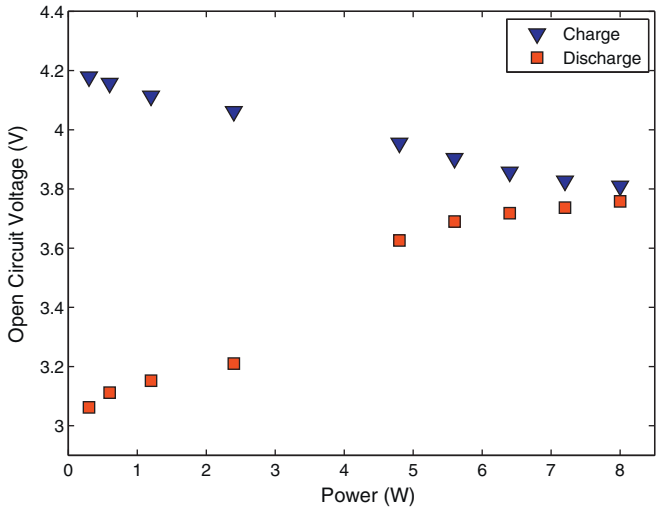


**Fig. 6.** Open-circuit voltages plotted for a single battery after 10 min rests. The converging voltages are evidence of undercharge and underdischarge.

In Fig. 7 we also compare our experimental internal efficiency data with our resistance-only models from Eqs. (16) and (17). We have changed our axes and units from those used in Fig. 2 to plot energy efficiency as a function of power. In terms of our earlier model, we are plotting a dimensionless energy efficiency $e$ as a function of power $P$ in units of watts. In order to make this adjustment, we must determine voltage $V$ and resistance $R$. $V$ is found by fixing the model's $y$-intercept at 0.98. The battery resistance $R$ is selected to fit the shape of our data; a slight difference between charge and discharge resistance is found to best fit the data, with discharge resistance approximately 10% higher. A lower resistance appears to fit the discharge data better at lower power, and a higher resistance at higher power, suggesting resistance may be dependent on power. Such a result is not surprising: resistance has been shown to vary both with C-rate and state-of-charge in lithium-ion batteries [16]. The state-of-charge effect may affect our resistance values because undercharge and underdischarge contribute to limited operational ranges for the batteries, and at high powers the batteries operate either in lower or higher average states-of-charge during charge or discharge, respectively.

Finally, we construct our complete energy–power model by combining the resistance-only model with our functional form for total available capacity, $Q(P)$. In Fig. 8 we plot the complete model including undercharge and underdischarge, the resistance-only model, and our experimental results. The complete model closely fits the experimental data, and the comparison to the resistance-only model suggests that undercharge and underdischarge dominate the shape of the energy–power curves. Although internal resistance losses on discharge show a greater loss in efficiency than internal losses on charge, this effect is small, and nearly negligible when compared to the impact of undercharge and underdischarge. Experimentally, we find that much less energy can be stored at high powers than discharged at high powers due to the reduction in available battery capacity imposed by voltage limits. The cells charged at a 10 C rate store on average only 38% of the maximum energy they can store at low powers, while cells discharged at 10 C provide 67% of the maximum energy they deliver at low power. When we compare these results to the internal efficiency data plotted in Fig. 7, we find that internal resistance contributes to about 14% of the reduction in energy stored in the battery at 10 C but 30% of the reduction in energy delivered from a battery discharged at 10 C. Undercharge and underdischarge are responsible for the remaining reduction in energy stored or discharged. The

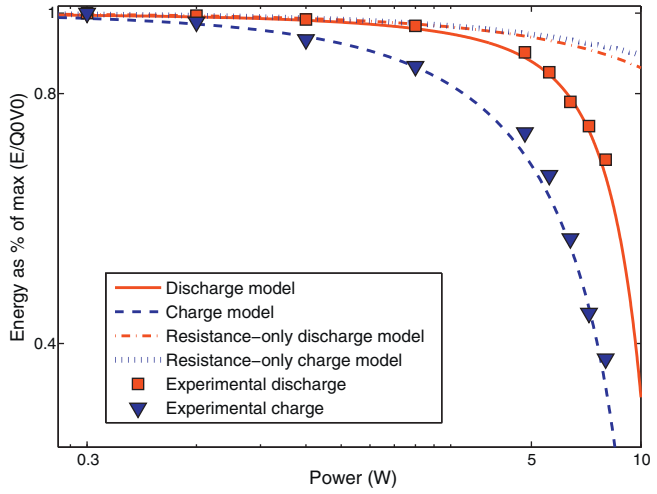


**Fig. 8.** Model for undercharge and underdischarge using experimentally determined value for $Q(P)$ as compared to models without undercharge and underdischarge. The experimental results are dominated by undercharge and underdischarge.

results suggest that moving voltage limits higher when charging at high power or lower when discharging may increase the available capacity of the battery, although we have not determined how far these limits can be moved without damaging the battery. The manufacturers' specifications for many battery chemistries suggest lower voltage limits on high-power discharge, but overcharging and overdischarging the battery should be avoided.

These models assume that the battery is being operated over the maximum possible range. However, underdischarge and undercharge are insignificant if a battery is being used predominantly in a small range near 50% state-of-charge. In this case, resistance losses would once again dominate the loss in energy stored or delivered, and at a given power charging may be slightly more efficient. Over the full battery range, however, we find that the range of charge powers is more limited than the range discharge powers. We expect that other battery chemistries with comparable voltage limitations would exhibit a similar response.

## 5. Conclusion

We model the trade-off between energy and power for battery charging and discharging using an equivalent circuit model and experimentally verify our results using lithium-ion cells. The model incorporates the effects of internal resistance losses and the impact of undercharge and underdischarge due to premature arrival at voltage limits. Resistance losses at any given power result in lower internal efficiency for discharge than charge. However, we find resistance losses to be small in lithium-ion cells compared to the loss of available capacity in the cell caused by voltage cutoffs. We determine the magnitude of undercharge to be much greater than underdischarge because of the shape of the voltage curve on charge and discharge. The voltage limit is located on a shallow portion of the charge curve, so a small shift upwards due to increased power results in a large reduction in the Ah throughput; the voltage limit on the discharge curve is located in a steep section, so the effect of an offset in the voltage curve has a much smaller impact on total discharge capacity. In lithium-ion batteries we therefore find a smaller total amount of energy can be stored at a given power than can be discharged at the same power, and that this effect is primarily caused by user-imposed voltage limits. However, we expect that if the same battery is operated over a small range of states-of-charge far from the voltage limits, it can be charged for short periods of time with higher internal efficiency than if discharged at the same power. In variable power systems, lithium-ion batteries can therefore be charged relatively efficiently at high powers near 50% state-of-charge, but cannot charge at high powers for as long as they can be discharged at high powers. Our approach can be extended to other battery chemistries as well, and will allow for the appropriate selection of a range of operating powers and the design of control systems for battery charge and discharge in variable systems.

## Acknowledgment

We would like to thank the Carbon Mitigation Initiative at Princeton University for supporting this work.

## References

[1] R. Marom, S.F. Amalraj, N. Leifer, D. Jacob, D. Aurbach, Journal of Materials Chemistry 21 (2011) 9938–9954.
[2] B. Scrosati, J. Garche, Journal of Power Sources 195 (2010) 2419–2430.
[3] V. Svoboda, H. Wenzl, R. Kaiser, A. Jossen, I. Baring-Gould, J. Manwell, P. Lundsager, H. Bindner, T. Cronin, P. Norgard, A. Ruddell, A. Perujo, K. Douglas, C. Rodrigues, A. Joyce, S. Tselepis, N. van der Borg, F. Nieuwenhout, N. Wilmot, F. Mattera, D.U. Sauer, Solar Energy 81 (2007) 1409–1425.
[4] A. Burke, Proceedings of the IEEE 95 (2007) 806–820.
[5] R. Cope, Y. Podrazhansky, 14th Annual Battery Conference on Applications and Advances, 1999, pp. 233–235.
[6] S.B. Peterson, J. Apt, J. Whitacre, Journal of Power Sources 195 (2010) 2385–2392.
[7] K. Divya, J. Østergaard, Electric Power Systems Research 79 (2009) 511–520.
[8] F.A. Amoroso, G. Cappuccino, Journal of Power Sources 196 (2011) 9574–9578.
[9] J. Viera, M. González, B. Liaw, F. Ferrero, J. Álvarez, J. Campo, C. Blanco, Journal of Power Sources 171 (2007) 1040–1045.
[10] J. Wang, SAE 2010 World Congress and Exhibition, SAE Paper No. 2010-01-1238, Detroit, MI, USA, April 2010.
[11] M.W. Verbrugge, R.Y. Ying, Journal of the Electrochemical Society 154 (2007) A949–A956.
[12] D. Ragone, Mid-Year Meeting of the Society of Automotive Engineers, Detroit, MI, May 20–24 (1968).
[13] T. Christen, M.W. Carlen, Journal of Power Sources 91 (2000) 210–216.
[14] T. Christen, C. Ohler, Journal of Power Sources 110 (2002) 107–116.
[15] M. Doyle, Y. Fuentes, Journal of the Electrochemical Society 150 (2003) A706–A713.
[16] J.-S. Hong, H. Maleki, S.A. Hallaj, L. Redey, J.R. Selman, Journal of the Electrochemical Society 145 (1998) 1489–1501.
[17] J. Gomez, R. Nelson, E.E. Kalu, M.H. Weatherspoon, J.P. Zheng, Journal of Power Sources 196 (2011) 4826–4831.
[18] M. Chen, G. Rincon-Mora, IEEE Transactions on Energy Conversion 21 (2006) 504–511.
[19] L. Gao, S. Liu, R. Dougal, IEEE Transactions on Components and Packaging Technologies 25 (2002) 495–505.
[20] Z. Salameh, M. Casacca, W. Lynch, IEEE Transactions on Energy Conversion 7 (1992) 93–98.